J Comp Physiol (1983) 152:79–90

Journal
of Comparative
Physiology · B

Intestinal glucose transport in carnivorous and herbivorous marine fishes

Ronaldo P. Ferraris[1] * and Gregory A. Ahearn[1] **
Department of Zoology, 2538 The Mall, University of Hawaii at Manoa, Honolulu, Hawaii 96822, USA

Accepted April 5, 1983

Summary. The influx and transepithelial movements of glucose and their effects on the electrophysiology and Na transport in upper and lower intestines of the herbivorous surgeonfish, *Acanthurus mata*, and carnivorous eel, *Gymnothorax undulatus*, were measured. The K_t^G and J_{max}^G of glucose influx into the tissues were higher in the surgeonfish upper intestine than in the surgeonfish lower intestine or in both segments of the eel intestine. A prominent diffusion-like transport component was also measured in all four segments during influx experiments. Net transepithelial glucose fluxes (0.05 mM) were greater in eel intestines than in those of the surgeonfish largely due to an apparent lower apical membrane permeability of the former coincident with reduced backflux of glucose from epithelium to lumen. All four stripped intestinal segments exhibited non-significant (from zero; $P>0.05$) or small, serosa-negative transepithelial potential differences (-0.1 to -2.2 mV), and low transepithelial resistances (40–88 Ω cm^{-2}). Each tissue displayed significant ($P<0.05$) serosa negative short-circuit currents and only the upper intestines in both fish showed net transepithelial fluxes of Na. Glucose addition to the mucosa did not significantly ($P>0.05$) change the transepithelial resistance, but did induce a significant ($P<0.05$), but slow reduction in serosa negative short-circuit current. Although 3 of the 4 intestinal segments exhibited increased J_{net}^{Na} with added luminal glucose, these increased net cation fluxes were not quite significant ($P>0.05$). It is concluded that coupled Na-glucose transport occurs in these tissues, but that metabolic enhancement of unrelated current-generating mechanisms also takes place and may modify depolarizing effects of organic solute transfer.

Introduction

Sugar transport has been extensively studied in the intestines of many terrestrial and freshwater organisms representing several vertebrate and invertebrate phyla (Goldner et al. 1969; Schultz and Curran 1970; White and Armstrong 1971; Kimmich 1981; Kimmich and Randles 1976; Ahearn and Maginniss 1977; Beames et al. 1977). Most of these animals possess a sodium-dependent secondary active transport system for sugars from lumen to blood that induces a significant change in transepithelial potential difference when the nutrient is added to the lumen (serosa becomes more electrically positive). Sugar influx across the apical membrane is thought to be coupled to sodium entry, while exit of sugar across the basolateral border occurs via a facilitated sodium-independent mechanism and that of sodium takes place via the Na-K-ATPase.

Similar studies involving marine organisms, particularly marine fishes, are limited in number. Most of the early transport experiments using marine fishes dealt mainly with transepithelial nutrient movements and subsequently, accumulation or lack of accumulation of these solutes in the submucosal or serosal fluids (Wilson 1957; Musacchia and Fisher 1960; Carlisky and Huang 1962; Rout et al. 1965; Musacchia et al. 1966; and Huang and Rout 1967). These early studies did not compare the effects of diet and feeding habits on organic solute influx characteristics, nor did they examine

* Present address: Aquaculture Department, Southeast Asia Fisheries Development Center, P.O. Box 256, Iloilo City, Philippines
** To whom offprint requests should be sent

Abbreviations: *SCC* short-circuit current; *PD* electrical potential difference; *ΔPD* glucose-evoked potential

the comparative contribution of upper and lower intestines to overall nutrient absorption. In addition, no study has yet examined the effects of nutrient absorption on intestinal electrophysiology and ion transport in marine fishes.

This study describes the role of epithelial cells in fish intestinal glucose absorption, and how various glucose transport parameters differ between carnivorous and herbivorous species. In addition, this study also examines the effects of glucose on electrophysiological properties of the teleost intestine.

Materials and methods

Collection and maintenance of animals. Surgeonfish (*Acanthurus mata*) and moray eels (*Gymnothorax undulatus*) (Fig. 1) were collected from coral reefs in Kaneohe Bay, Oahu, Hawaii by trapping. They were fed and maintained in submerged cages for several days before being transported to the laboratory where they were kept in closed-system aquaria and starved for about 48 h before experimentation.

Incubation media for isolated fish intestines. The ionic composition and osmolarity of the incubation medium was based on measurements of the constituents of blood samples and intestinal fluids taken from freshly collected fish. This medium had the following salt concentrations in mM: NaCl, 150; KCl, 4; $CaCl_2$, 4; Na_2SO_4, 4; KH_2PO_4, 1.2; $MgSO_4$, 1; and $NaHCO_3$, 10. Mean osmolarity and pH values (± 1 standard error), after bubbling with 98% oxygen/2% carbon dioxide mixture, were 330 ± 2 (10) mOsm/kg and 7.3 ± 0.1 (15), respectively (numbers in parentheses represent sample size). The solutions bathing the mucosal and serosal sides of the tissue were both gassed and stirred by a continuous stream of 98% oxygen/2% carbon dioxide mixture for about 15 min prior to and during experimentation. In related experiments, this particular saline was found to maintain a steady state transepithelial potential difference across eel and surgeonfish intestinal preparations for 3 to 6 h at 24 °C, suggesting that tissue integrity and viability were maintained throughout this period.

Definition of intestinal segments. Fish were killed either by a blow to the head (surgeonfish) or by decapitation (eel). The intestines were then removed, placed in cold saline (3–5 °C), divided into separate segments and slit open. Surgeonfish upper intestine (Fig. 1, upper photograph) was defined in this study as the first 8–12 cm after the stomach while the lower intestine was defined as the last 6–12 cm of gut before the anal opening. Morphological markers served to demarcate one segment from others. Eel upper, middle and lower intestines were easily distinguished from one another (Fig. 1, lower photograph). The eel upper intestine had deep mucosal intestinal folds which were much shallower in the middle intestine, which in turn, was separated from the lower intestine internally by a valve. Preliminary

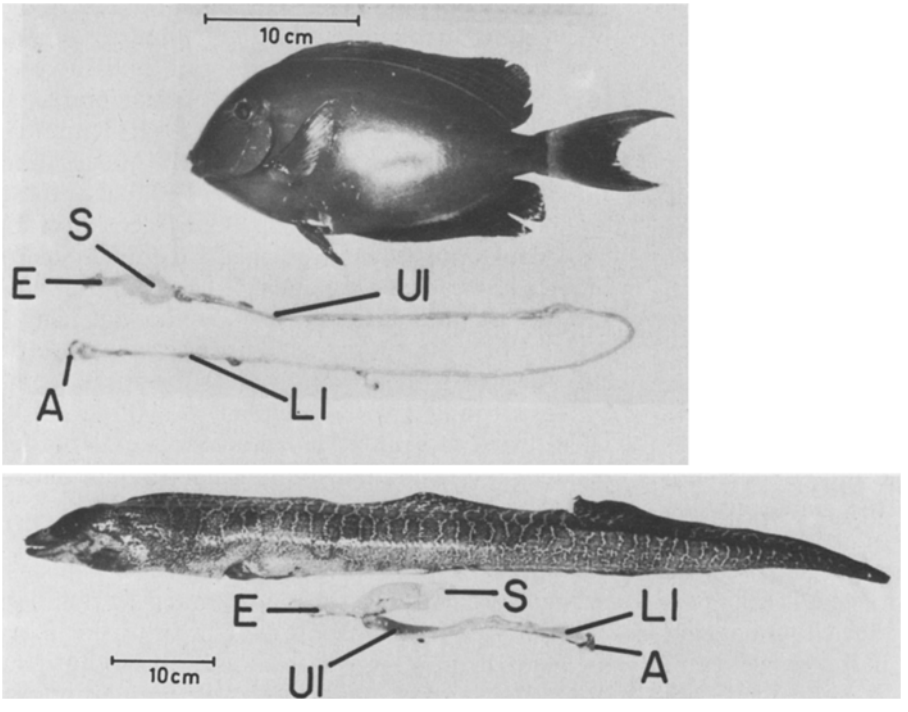

Fig. 1. General morphology of carnivorous and herbivorous marine fishes used in this study and their digestive tracts. *E* esophagus; *S* stomach; *A* anus; *UI* upper intestine; *LI* lower intestine. *Upper photograph:* The surgeonfish has a long intestine which, in vivo, is highly coiled and wound around itself and the stomach, forming a compact mass in the abdominal cavity. The total length of the intestine is around 60 times the intestinal diameter and about 2.3 times the standard length of the fish. The upper and lower intestines as defined in this study each comprise about a quarter of the intestinal length. Calibration bar: 10 cm. *Lower photograph:* The eel intestine is a straight tube extending from its connection with the stomach to the rectum. The total length of the intestine is approximately 16 times the intestinal diameter and 0.33 times the standard length of the fish. The upper intestine comprises abut a third and the lower intestine a sixth of the total intestinal length. Calibration bar: 10 cm

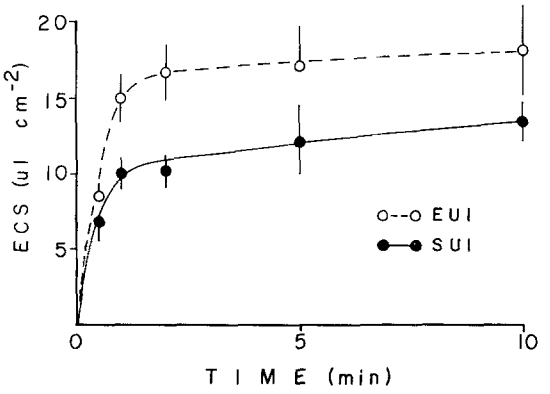

Fig. 2. Extracellular space (*ECS*) of the eel (*EUI*) and surgeonfish (*SUI*) upper intestines. ECS was estimated in the intestinal mucosa by incubating the luminal side of the tissue for different lengths of time with ^{3}H-mannitol. Each *circle* represents the mean of at least five derminations. *Vertical bars* represent ± 1 SE. Absence of SE bars indicates that the statistical variability lies within the area of the plotted point. The eel and surgeonfish lower intestines had curves similar to that of the SUI

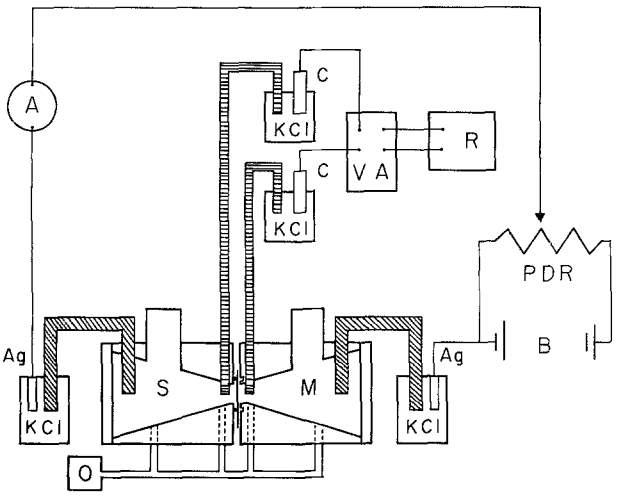

Fig. 3. Experimental apparatus used to measure transmural electrical potential difference and sodium fluxes across eel and surgeonfish intestines. Saturated KCl-agar salt bridges (thin with horizontal lines) connected both mucosal (*M*) and serosal (*S*) media via 3 M KCl solutions and calomel electrodes (*C*) to voltage amplifier (*VA*)-dual pen recorder (*R*) complex for potential difference (*mV*) estimations. Saturated Ringer-agar salt bridges (thick with diagonal lines) connected both M and S media via 3 M KCl solutions and Ag – AgCl electrodes (*Ag*) to a microammeter (*A*)-battery (*B*)-potential divider (*PDR*) complex through which an external electromotive force was applied. During short-circuit current applications, the external electromotive force was supplied from B and with the aid of the PDR, the voltage was adjusted so that the potential difference across the intestine, as read in R, was zero. Throughout the entire experiment, 4 inlets from a 98% oxygen/2% carbon dioxide tank (*O*) served to stir and oxygenate the solution bathing the intestine

experiments showed that rates of glucose uptake did not vary significantly among 3 cm^2 pieces of tissues taken from different sections within the same upper or lower segment.

Influx experiments. Rectangular pieces of tissue (2.5–4.0 cm^2) were mounted as sheets in modified Ussing chambers. The area of tissue exposed to the bathing solution was 0.2 cm^2 (serosal surface). Initial experiments showed that solute uptake was linear for at least 2 min in all four tissues. One minute was chosen as the standard incubation time in subsequent experiments. Within this time interval, glucose activity in the serosal solution was not significantly different from control.

At the beginning of an experiment, a concentrated solution (20–50 µl) of labelled [2-^{3}H(N)] (New England Nuclear, Corp.) and unlabelled D-glucose was added to the mucosal side to make a final concentration of 0.5–1.0 µCi labelled solute per ml of saline; a final concentration of 0.01–25 mM unlabelled solute, and a final volume of 2 ml per chamber. Following incubation, the tissues were removed and rinsed rapidly (about 1 s) in ice-cold saline, extracted for at least 24 h in 5 ml of 80% ethanol, then counted in a liquid scintillation spectrometer (Beckman LS-8100). In some experiments, the ethanol extract was checked for volatile (probably ^3H_2O) activity while the remaining tissues were examined for ethanol insoluble activity (bound activity). Labelled compounds in ethanol extracts were separated and identified by thin-layer chromatography on plastic silica gel and cellulose sheets (Eastman Kodak Co. and EM Laboratories, Inc.).

Mannitol and inulin spaces were monitored during influx (0.5 to 10 min). These spaces were used as an estimate of extracellular space and labelled glucose restricted to them was subtracted from total radioactivity incorporated by the tissue to yield cellular uptake alone. Representative examples of mannitol uptake in the eel and surgeonfish upper intestines are shown in Fig. 2. Mannitol extracellular spaces (in µl cm^{-2}) for each tissue were: (1) surgeonfish upper intestine: 9.6 ± 1.1; (2) surgeonfish lower intestine: 10.8 ± 1.1, (3) eel upper intestine: 15.4 ± 2.4; and (4) eel lower intestine: 10.3 ± 1.8.

Transmural transport. The serosal and external muscle layers were stripped from the mucosa. Unidirectional transepithelial solute fluxes across the intestinal sheets were then measured simultaneously in paired preparations with similar transepithelial resistances. A concentrated solution (300 or 500 µl) of labelled and unlabelled material was added to 5.7 or 9.5 ml of bathing solution to make a final concentration of 0.05 mM and a ratio of 1 µCi of tritiated organic solute per ml of bathing solution. The entire preparation was allowed to reach steady state for about 20 or more minutes (when flux started to become a linear function of time) before the first sample was removed from the initially unlabelled side. Subsequent total activity samples were removed at 10 min intervals for 1.3 to 2.0 h and counted as previously described. Total counts in the initially unlabelled chamber at the final sampling period did not exceed 1% of the total counts in the initially labelled chamber.

Fluids for thin layer chromatography from the mucosal and serosal chambers were desalted by precipitation and centrifugation in cold (0 °C) 90% acetone. Acetone treatment was repeated 2 or 3 times. To monitor possible losses of acetone-soluble metabolites, desalting was also done with cold 96% ethanol. A few transmural transport experiments and thin layer chromatographic analyses were also done using D-[^{14}C(4)]-glucose (New England Nuclear, Corp.). Thin layer chromatography in these experiments was made in a manner similar to that for tritiated glucose experiments.

Electrophysiology and sodium fluxes. Electrical and ion flux studies were based on the methods of Clarkson and Toole (1964). The experimental apparatus is shown in Fig. 3. Potential offset between the two electrodes was minimized by pre-equilibrating

them with the appropriate bathing solution for about two hours before the experiment. The resistance of the fluid medium and the fluid displaced by the tissue was measured and taken into account for both electrical potential difference (PD) and short-circuit current (SCC) measurements.

A current-PD relationship was made by injecting a current (up to 120 $\mu A\ cm^{-2}$, depending on the tissue) across the stripped intestine and measuring the resultant PD at the beginning and end of each run to check whether tissue resistance changed over time. Spot checks for resistance alterations in the middle of the experiment were made by dividing the open circuit potential by the SCC. After the tissues reached electrical steady state, glucose was added to the mucosal aspect. If the concentrations placed into the mucosal solution were more than 2 mM, a corresponding concentration of D-mannitol was placed into the serosal solution to minimize streaming potentials. Control Ringer was added to both sides of the chamber at the end of each run to monitor changes from initial steady state.

In control Na flux experiments, non-labelled solutions were used to attain steady state PD and SCC values (30–60 min) in the paired preparations. Then, a current-voltage plot was made followed by the addition of a trace amount of ^{22}Na directly to one side of the chamber (1 $\mu Ci/ml$). After equilibration, samples were removed periodically from the initially unlabelled chamber to determine control unidirectional fluxes. To test for the effects of luminal organic solutes on transmural sodium fluxes, 2 mM glucose was added to the mucosa of both paired preparations. After a few minutes to allow the tissues to reach steady state, sampling was resumed as above. Experiments with the final samples taken from the unlabelled side with counts greater than 1% of the initial counts in the labelled chamber were rejected. Experiments where tissues changed their resistance by more than 20% were also rejected.

Results

Comparative morphology and diet

In teleosts it is known that the length and conformation of the intestine generally varies with food habits and individual diet (Bond 1979). These generalities were also disclosed in the present investigation. The moray eel possessed a very short intestine relative to body length and intestinal diameter (Fig. 1). In contrast, adaptations such as a gizzard-like stomach for grinding plant cells and increased intestinal length for prolonging retention time of food were found in the surgeonfish (Fig. 1).

Time course of nutrient uptake

The time course (30 s to 4 min) of 7.5 mM ^{3}H-D-glucose entry into the epithelium of eel and surgeonfish upper intestines is shown in Fig. 4. Over an incubation interval of 0.5 to 2.0 min, glucose uptake into both gut tissues was a linear function of time. Vertical intercepts were not significantly different from zero ($P > 0.05$). On the basis of these results a 1 min exposure time was selected for all influx determinations, because over this time period backflux of accumulated solute from cell to luminal medium was assumed to be minimal.

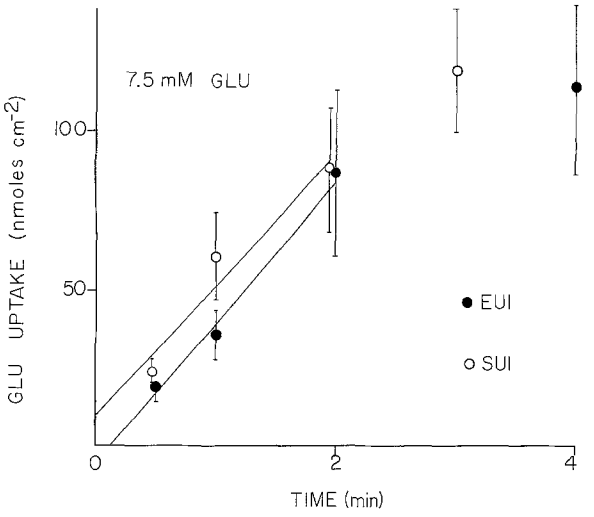

Fig. 4. Time course of 7.5 mM ^{3}H-D-glucose uptake across the apical border of epithelia from eel upper intestine (*EUI*) and surgeonfish upper intestine (*SUI*). Each *symbol* represents the mean of 3 to 4 determinations ±SE

Effects of external glucose concentration on glucose influx

Glucose influx into the mucosa of isolated upper and lower intestines of eel and surgeonfish was a curvilinear function of glucose concentration at low sugar concentrations, while a linear relationship occurred between the variables at high concentrations. A representative example showing surgeonfish upper intestinal glucose influx is presented in Fig. 5. Sugar influx of the four tissues could be described as the sum of two independent processes operating simultaneously: (1) a carrier-mediated transport system exhibiting saturation kinetics of the Michaelis-Menten type: and (2) a linear entry process having a rate that was proportional to the external sugar concentration. The combination of these two systems is defined by the equation:

$$J^G_{mc} = \frac{J^G_{max}[G]}{K^G_t + [G]} + k^G_d[G] \quad (1)$$

where J^G_{mc} is total glucose influx in nmoles cm^{-2} min^{-1}; J^G_{max} is maximal carrier-mediated influx; K^G_t is the sugar concentration resulting at 0.5 J^G_{max}; [G] is the external glucose concentration; and k^G_d is the rate constant of the linear entry process. Least squares regression analysis was used to determine the slope of the linear portion of glucose influx. This slope, or k^G_d, was then multiplied by

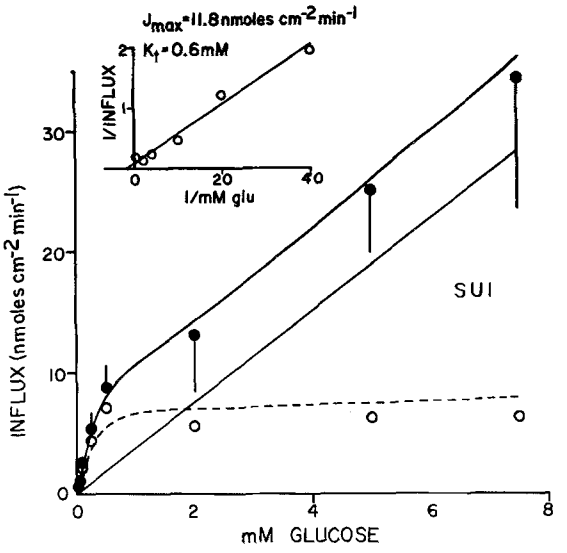

Fig. 5. ^{3}H-D-glucose influx across the apical border of the SUI epithelium as a function of glucose concentration in the mucosal medium (*solid circles*). During each experiment, the intestinal mucosa was exposed to radioactive glucose for 1 min. Each *solid circle* represents the mean of 4–6 determinations, while *vertical bars* are ±1 SE. The *continuous curved line* represents the total influx. The *continuous straight line* represents estimated influx due to the non-saturable component at different luminal glucose concentrations. *Interrupted curve and open circles* represent the estimated influx due to the saturable component. *Inset* is a Lineweaver-Burk plot of the estimated saturable influx component (*open circles*). Kinetic constants were estimated from the negative reciprocal of the x-intercept (K_t) and the reciprocal of the y-intercept (J_{max})

the concentration used and the product subtracted from the total uptake at each concentration to yield the saturable uptake component. The dashed line in Fig. 5 represents an estimate of the saturable portion of sugar influx for each gut segment. The transport constants, K_t^G, J_{max}^G, and k_d^G for all gut segments, are summarized in Table 1. The surgeonfish upper intestine had the highest K_t^G and J_{max}^G values, while the eel lower intestine appeared unique in having the lowest k_d^G. In the concentration range from 0.01 to 5.0 mM, non-saturable transport represented about 10–75% of total influx, implying that it played a significant role in influx of some food components at physiological concentrations.

Identification of total tissue radioactivity components following influx

Thin layer chromatography of ethanol extractable activity for each tissue segment following 1 min of mucosal exposure to ^{3}H-glucose, in most instances, yielded a single radioactivity peak with an R_f corresponding to that of standard glucose.

Table 1. Kinetic constants of ^{3}H-D-glucose influx into marine teleost intestines. Values were derived from kinetic analyses on each gut segment using methods outlined on Fig. 5 and discussed in the text

Intestinal segment	K_t^G (mM)	J_{max}^G (nmoles cm^{-2} min^{-1})	J_d^G (nmoles cm^{-2} min^{-1} mM^{-1})
Surgeonfish			
Upper intestine	0.6	11.8	3.8
Lower intestine	0.4	1.7	4.3
Eel			
Upper intestine	0.3	3.7	3.9
Lower intestine	0.3	2.4	1.0

While minor peaks appeared in some instances, only one of these minor peaks represented more than 4.5% of the total activity so that almost all non-volatile activity could be attributed to ^{3}H-glucose.

Ethanol extracted tissue samples exhibited about 50% volatile radioactivity in all intestinal segments suggesting possible metabolism and partial conversion of ^{3}H-glucose to tritiated water during the incubation period. After 1 min incubation time in glucose, ethanol insoluble activity in each tissue amounted to less than 5% of total activity.

Transepithelial glucose fluxes

Thin layer chromatography of the serosal fluid following mucosa to serosa flux of 0.05 mM ^{14}C-D-glucose showed that about 70 to 100% of the activity transported across the epithelium to the blood side was glucose. Thin layer chromatograms of fluids from the desalting process using ethanol were similar to those from acetone, indicating that the acetone treatment did not significantly discriminate against acetone-soluble glucose metabolites. Thin layer chromatography of mucosal fluids following serosa to mucosa flux of 0.05 mM ^{14}C-D-glucose showed 95% or greater glucose activity. All transmural fluxes of labelled glucose subsequently discussed in this report were estimated after subtraction of non-glucose radioactivity and therefore represent unidirectional and net movements of the sugar only.

Table 2 describes transmural fluxes of 0.05 mM glucose in surgeonfish and eel intestines. Except for the surgeonfish lower intestine, significant movements of glucose toward the blood were found ($P<0.05$). Larger glucose fluxes occurred in eel tissue than in comparable intestinal segments from the surgeonfish. The J_{ms}^G and J_{net}^G glucose

Table 2. Transepithelial ^{3}H-D-glucose fluxes across marine teleost intestines. Fluxes were determined using stripped, paired preparations of adjacent tissues and a glucose concentration of 0.05 mM. Values are means of 5 experiments ±1 SE

Intestinal segment	J^G_{ms}	J^G_{sm} (pmoles cm^{-2} min^{-1})	J^G_{net}
Surgeonfish			
Upper intestine	23±7	2±1	21±7
Lower intestine	7±2	3±1	4±2
Eel			
Upper intestine	59±14	1±0	59±14
Lower intestine	289±57	6±3	284±52

fluxes, however, were higher in the surgeonfish upper than in the lower intestine ($P<0.05$). The least amount of serosa to mucosa glucose flux was found in the eel upper intestine, the tissue with the highest transepithelial electrical resistance (see below).

Effects of D-*glucose on intestinal transmural potential difference*

The spontaneous steady state transmural potential difference and resistance recorded across isolated stripped eel upper intestine were −1.58±0.16 mV ($n=17$), serosa negative, and 88±5 ohms cm^{-2} ($n=29$), respectively. Both electrical parameters were significantly different ($P<0.05$) from those in both gut segments of the surgeonfish (below) and in the eel lower intestine which had a PD of −2.24±0.33 mV ($n=19$), serosa negative, and a tissue resistance of 59±5 ohms cm^{-2} ($n=18$).

Luminal addition of D-glucose to eel lower intestine resulted in a gradual, slow decline toward zero of the serosa negative PD (Fig. 6). This decline was much slower to develop than the glucose-evoked potential changes reported in the rabbit ileum (Schultz and Zalusky 1964), sea hare gut (Gerencser 1978), and goldfish intestine (Smith 1966; Albus and van Heukelum 1976). The relationship between glucose concentration and the ΔPD in both eel tissues was hyperbolic (Fig. 7) so that the following equation describes the effects of glucose on teleost intestinal electrophysiology:

$$\Delta PD = \frac{\Delta PD^G_{max}[G]}{K^G_t + [G]} \quad (2)$$

where ΔPD is glucose-evoked change in transmural potential difference, ΔPD^G_{max} is maximal glucose-evoked change in PD, K^G_t is glucose concentration resulting in 50% ΔPD^G_{max}, and [G] the luminal glucose concentration. The kinetic constants of this relationship (Table 3) were obtained by linear regression using a Lineweaver-Burk plot of 1/[G] vs. 1/ΔPD (example in Fig. 7). Tissue resistance did not change significantly after luminal glucose addition.

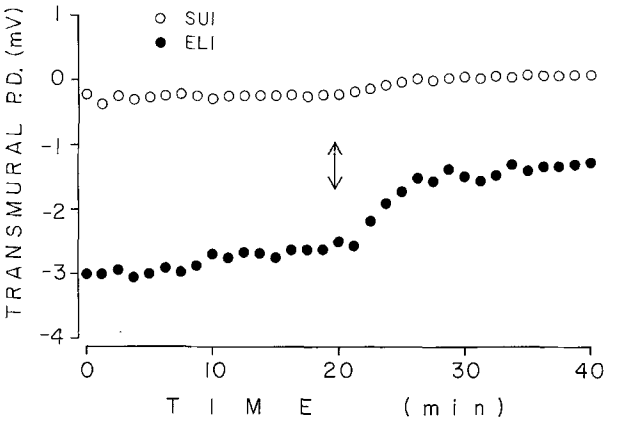

Fig. 6. Effects of 2 mM D-glucose on the transmural potential difference across surgeonfish upper intestine (*SUI*) and eel lower intestine (*ELI*). Polarity values refer to serosa relative to lumen. *Circles* refer to results from a single experiment with the gut initially placed in control saline (both sides) followed by mucosal exposure to saline with glucose. *Arrows* correspond to the time when 2 mM glucose was added to the mucosal chamber. The glucose-evoked potential is the difference between the steady state PD after glucose addition and steady state control PD

Table 3. Kinetic constants of glucose-evoked changes in the transepithelial electrical potential difference across surgeonfish and eel intestines. Values were derived from kinetic analyses of each gut segment using methods outlined in Fig. 7 and discussed in the text. Surgeonfish lower intestine did not respond to luminal addition of D-glucose

Intestinal segment	K^G_t (mM)	ΔPD^G_{max} (mV)
Surgeonfish		
Upper intestine	0.3	0.2
Eel		
Upper intestine	0.1	0.4
Lower intestine	0.1	0.7

In the surgeonfish when both gut surfaces were bathed in normal medium, a small spontaneous transmural potential difference that was not significantly different from zero was recorded for upper intestine (−0.11±0.08 mV ($n=28$); serosa negative). This result was significantly different ($P<0.005$) from the surgeonfish lower intestinal serosa negative transmural PD of −0.62±0.01 mV ($n=23$) obtained under identical experimental conditions. Tissue resistances of the stripped upper intestine (40±3 ohms cm^{-2} ($n=13$)) and lower intes-

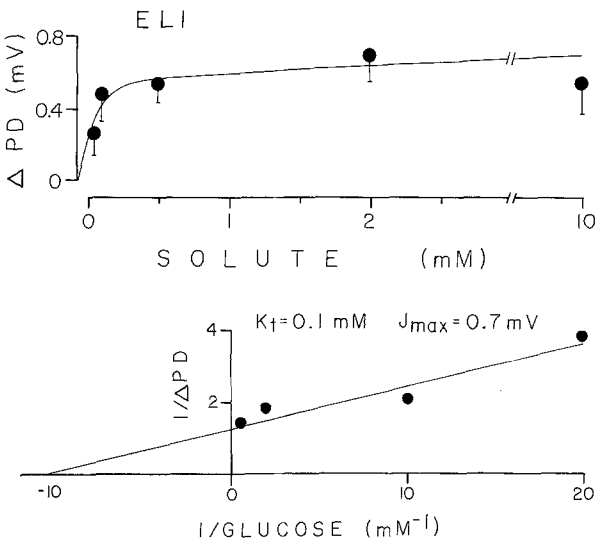

Fig. 7. *Upper panel:* Effect of luminal glucose concentration on control transepithelial potential difference (serosa negative) in the eel lower intestine. Each *symbol* represents the mean of at least five determinations. *Vertical bars* are ±1 SE. The tissue was incubated for 20 to 30 min prior to and after addition of the nutrient to ensure steady state in control and test conditions. *Lower panel:* Lineweaver-Burk plot of mean glucose-evoked potentials from the upper panel. Transport constants were estimated from the negative reciprocal of the x-intercept (K_t) and the reciprocal of the y-intercept (J_{max})

tine (42±4 ohms cm^{-2} (n=23)) were not significantly different ($P>0.05$), suggesting that the latter tissue has a greater current-generating transmural ion transport capacity.

In surgeonfish upper intestine, luminal addition of 0.05 to 10 mM D-glucose did not significantly change tissue resistance, but resulted in a small, very slow increase in the transmural PD (becoming more serosa positive). The generation of *ΔPD*, from the time of luminal glucose addition to the time when *ΔPD* peaked, took at least 5 min (Fig. 6). Removal of glucose from the gut lumen resulted in a slow decrease toward control *PD*. Luminal addition of glucose in the surgeonfish lower intestine had no significant effect on tissue resistance and transmural *PD*.

Effects of glucose on transepithelial sodium flux and SCC

Under SCC conditions, a significant ($P<0.05$) net Na flux from mucosa to serosa occurred across fish upper intestine, suggesting active transport of this ion (Table 4). Because the open circuit potential became more positive with glucose, the effect of glucose on this net Na flux under SCC condi-

Table 4. Transepithelial sodium fluxes under control short-circuit conditions. Values are means±1 SE. Fluxes were determined with stripped, paired preparations of adjacent tissues. Polarity refers to serosa relative to mucosa, so that a positive J^{Na}_{net} indicates net sodium movement to the serosa

Intestinal segment	n	J^{Na}_{ms}	J^{Na}_{sm}	J^{Na}_{net}	*SCC*
		(nmoles cm^{-2} min^{-1})			
Surgeonfish					
Upper intestine	5	224±18	176±16	48± 9*	− 2.5±1.6*
Lower intestine	5	218±21	236±35	−18±39	−13.9±1.4*
Eel					
Upper intestine	4	62±11	27± 5	36±11*	− 8.1±1.7*
Lower intestine	5	175±18	163±11	12±10	−20.7±3.6*

* Significantly different from zero ($P<0.05$)

Table 5. Transepithelial sodium fluxes under short-circuit conditions following mucosal addition of 2 mM D-glucose. Values are means ±1 SE. Fluxes were determined with stripped, paired preparations of adjacent tissues. *ΔSCC* is the difference between SCC after glucose addition (this table) and control SCC (Table 4). Polarity refers to serosa relative to mucosa

Intestinal segment	n	J^{Na}_{ms}	J^{Na}_{sm}	J^{Na}_{net}	*SCC*	*ΔSCC*
		(nmoles cm^{-2} min^{-1})				
Surgeonfish						
Upper intestine	5	256±20	180±17	76±16*	− 0.6±1.8	2.0±0.4*
Lower intestine	7	198± 8	212±14	−14±17	−14.5±1.6	−0.7±0.5
Eel						
Upper intestine	4	104± 4	53±10	52±17*	− 6.8±1.6	1.3±0.3*
Lower intestine	5	201±22	170±10	32±15*	−17.6±3.3	3.2±0.6*

* Significantly different from zero ($P<0.05$)

tions was studied. The magnitudes of the SCC's in the control condition (Table 4) were indicative to the magnitudes of the open circuit PD's of the respective tissues.

Addition of glucose to the lumen of these tissues induced a small decrease in serosa negative SCC and a small increase in net serosally-directed Na flux (Table 5). While flux changes were not statistically significant ($P > 0.05$), the difference between the SCC's under control conditions and after glucose addition (Δ SCC's; Table 5) were significantly different from zero ($P < 0.05$).

Discussion

Glucose influx into surgeonfish and eel intestines

Transport pathways

Glucose influx in moray eel and surgeonfish intestines occurred by two independent mechanisms. At relatively low luminal solute concentrations, the majority of sugar entry occurred across the apical cell membrane by carrier processes exhibiting Michaelis-Menten kinetics. At high luminal nutrient concentrations (greater than 1 mM), the carrier mechanisms approached saturation and the majority of solute influx was due to non-saturable transport. Non-saturable influx might be a result of simple solute diffusion across the mucosal cell border or carrier transfer by mechanisms that did not show saturation within the concentration range utilized. Composite influx kinetics for organic solutes, including Michaelis-Menten properties and non-saturable transfer, were also found for valine in goldfish (Kitchin and Morris 1971), for leucine in rainbow trout (Ingham and Arme 1977), and for cycloleucine in killifish (Miller and Kinter 1979).

Saturable solute influx

The differences between the kinetic constants of surgeonfish and eel upper intestines (Table 1) suggest that in the former, luminal concentrations of glucose might be somewhat higher than those in the eel. Quantitative analyses of gut contents in the surgeonfish showed mainly partially digested algal (generally chlorophytes and chrysophytes) materials. No study has yet been done on the behavioral feeding characteristics of *A. mata*, but Ogden and Lobel (1978) reported that *Acanthurus triostegus* preferred a green alga, *Enteromorpha* sp., as food. Bardach et al. (1972) reported that fresh *Enteromorpha intestinalis* contains 8.5% carbohydrate and 3.7% protein (wet weight). On the other hand, gut contents of some freshly caught moray eels consisted only of fish. Because such meals are composed of about 14% protein and only trace amounts of carbohydrates (Bardach et al. 1972), the intestine of *G. undulatus* would probably contain a much lesser amount of sugars than that of the surgeonfish.

Although it is not entirely clear whether the intestinal enzyme concentrations of fish are adapted to diet (Kapoor et al. 1975; Hofer 1979a, b), most fishes can digest starch to glucose to some extent (Cowey and Sargeant 1979) and herbivores tend to digest a much greater percentage than do carnivores (about 85% for carp, Chiou and Ogino 1975). Furthermore, amylase concentrations in fish were shown to increase in quantity when carbohydrate in the diet was increased (Nagase 1964). The surgeonfish therefore probably not only consumes more carbohydrates in terms of quantity and composition of diet, but might also be able to digest a greater proportion of a starchy meal than most carnivores. This might explain the comparatively low affinity, but high capacity, transport system for glucose in surgeonfish upper intestine.

Karasov and Diamond (1981) compared intestinal transport and uptake of glucose per cm^2 (serosal surface area) in rats, mice, and lizards fed carnivorous and omnivorous diets, and found that these parameters appeared highest when the supplied dietary glucose level was elevated. This finding corroborates the higher upper intestinal J^G_{max} value for the herbivore than that of the carnivore found in the present study.

Table 1 shows that the K^G_t of glucose transport was less in surgeonfish lower intestine than in upper intestine. In both fishes, the J^G_{max} of glucose transport was less in the hindguts. No other study has compared the influx of glucose, or any other sugar, in upper and lower fish intestines. However, using similar methods and glycine as substrate, Boge et al. (1979) found that K_t's were much lower in the hindgut of the rainbow trout than in the foregut. These investigations imply an scavenger function in the lower intestines, transporting what might remain from upper intestinal absorptive activities.

Non-saturable solute influx

Eel and surgeonfish intestine displayed non-saturable glucose influxes which were about one-half those of alanine (Ferraris 1982). Similar findings were reported by Huang and Rout (1967) who re-

ported a non-saturable component of D-galactose transport into killifish intestine which was less than that of tryptophan. The k_d^G values for moray eel and surgeonfish gut (Table 1) are similar to those for other fishes in the literature (Huang and Rout 1967, our estimates; Kitchin and Morris 1971; Ingham and Arme 1977; Miller and Kinter 1979). These previously reported K_d values ranged from 1.7 to 9.7 nmoles cm^{-2} min^{-1} mM^{-1}, while those of glucose and alanine in moray eel and surgeonfish ranged from 1.0 to 10.0 nmoles cm^{-2} min^{-1} mM^{-1} (Table 1; Ferraris 1982). In another study which did not present a K_d value for solute influx in trout midgut (Boge et al. 1979), a calculated estimate of this parameter from their data was 4.6 nmoles cm^{-2} min^{-1} mM^{-1}.

The biological significance of this component is not clear. This non-saturable entry might have evolved as a consequence of salinity adaptation since K_d's seem to be higher or present in more saltwater fish species than in freshwater species (Ferraris 1982). Intestines of seawater-adapted individuals of euryhaline species were shown to possess lower transepithelial resistances and experience general increases in the following: (a) ionic permeability; (b) osmotic permeability to water; and (c) the molar ratio of water to sodium in the fluid moving across the intestinal wall, when compared to freshwater-adapted individuals (Oide and Utida 1967; Utida et al. 1967; Skadhauge 1974; Ando 1975). These changes suggest an increase in the number of aqueous membrane pores or a less hydrophobic membrane, which might explain the existance of a significant K_d in these fishes.

The relative low permeability (k_d^G) of glucose in epithelial cells of eel lower intestine might be due to a higher concentration of divalent cations such as Mg (Shehadeh and Gordon 1969) and Ca in this location which could decrease membrane permeability by affecting surface charge. Calcium concentrations tended to be greater in the lower intestinal lumen of eels (6.7 ± 0.8 mM; 3 guts) than in the pooled luminal calcium concentrations from whole intestines (5.3 ± 0.4; 9 guts). Only Boge et al. (1979) studied the kinetics of uptake in fish lower intestine, and it could be deduced from their figures that a non-saturable component of uptake was present; their failure to correct for this resulted in a very high K_t for glycine (11 mM) in this location. If a K_d from their Fig. 3 were estimated as had been explained above, it would be 1 nmole cm^{-2} min^{-1} mM^{-1} as compared to 4.6 nmoles cm^{-2} min^{-1} mM^{-1} for the upper intestine in the same fish, a pattern consistent with that found for eel intestine in the present investigation.

Transepithelial glucose fluxes

Results of transepithelial flux studies, using the relatively low luminal glucose concentration of 0.05 mM, showed that more net sugar movement occurred across eel intestine than occurred across that of the surgeonfish (Table 2). This considerable net glucose flux in the eel was the consequence of a far larger unidirectional mucosa to serosa sugar transfer in this fish than the comparable flux in the surgeonfish. As indicated in Table 1, both glucose influx K_t^G and J_{max}^G were generally lower in the eel than in the herbivore. Using the kinetic constants in this table for surgeonfish upper intestine and those for both upper and lower eel intestines in equation (1) at a glucose concentration of 0.05 mM, it is clear that unidirectional transmembrane influx in the upper herbivore intestine significantly exceeds that for both parts of the carnivore gut.

The apparent diffusion constant (k_d^G) for surgeonfish upper intestine is four times that of the eel lower intestine (Table 1). While this transport component may facilitate the downhill flow of sugar from lumen to cell during conditions of low intracellular glucose concentration, it also would lead to the loss of accumulated intracellular sugar across the mucosal membrane if luminal glucose concentrations were low. Therefore, while surgeonfish upper intestine exhibits influx kinetic constants which lead to more rapid transfer of sugar from the lumen to cell, it also possesses a large apparent diffusion process in the brush border that appears to result in the significant backflux to the lumen of much accumulated cellular glucose. The overall effect of this combination in the surgeonfish upper intestine is that net mucosa to serosa transepithelial flux of this sugar is 13 times less than that occurring in the eel lower intestine possessing the small apparent diffusion component.

Quantitatively, the transepithelial glucose transport rates reported in this paper for eel and surgeonfish (4–290 pmoles cm^{-2} min^{-1}) are in general agreement with values published in the literature for fishes by Musacchia et al. (1966), Cartier et al. (1979), and Naftalin and Kleinzeller (1981), when these earlier values are transformed to similar units and when corrected for differences in substrate concentration (11–210 pmoles cm^{-2} min^{-1}).

Electrophysiology of intestinal glucose and sodium absorption

Effects of glucose on the transepithelial electrical potential difference across freshwater fish intestine

was studied by Smith (1966) and Albus and van Heukelem (1976) who reported that addition of glucose to the mucosal surface of the goldfish intestine resulted in a rapid (0.5 min to 50% ΔPD) and marked change of 1.7 to 2.5 mV in the transmural PD. Glucose addition to surgeonfish and eel intestine however resulted in a delayed, relatively slow (5 min to 50% ΔPD) PD response of a smaller magnitude (0.2 to 0.7 mV; Fig. 6). The concentration of glucose that produced half maximal ΔPD (K_t^G's) in the marine fishes used in this study (Table 3) were similar, however, to the K_t^G of 0.2 mM observed in goldfish by Smith (1966). The electrophysiologically derived K_t^G's in surgeonfish and eel intestines (Table 3) had a pattern similar to that seen in influx experiments (Table 1) in that affinity constants for glucose were higher in herbivorous fish intestine.

Like other leaky epithelia, the resistances of small intestines from terrestrial vertebrates are low, ranging from 80 (hamster) to 350 (turtle) ohms cm^{-2} (Haang and Chen 1975). Transepithelial resistances of intestines from marine fishes are generally even lower. Ando et al. (1975) showed that in seawater-adapted individuals, intestinal resistances of rainbow trout and the eel, *Anguilla japonica*, were 43 and 60 ohms cm^{-2}, respectively, and were significantly less than those from freshwater-adapted individuals (same fishes; 108 and 88 ohms cm^{-2}). In leaky epithelia, this low resistance is generally due to paracellular and junctional complexes that offer little resistance to ionic flow, reducing the ability of the tissues to generate high transmural PD's. The surgeonfish intestines displayed one of the lowest transepithelial resistances known (approx. 40 ohms cm^{-2}), and this could be one primary reason why only low transmural *PD*'s are generated across it and why addition of organic solutes like glucose hardly modify the existing transepithelial potential. On the other hand, the eel intestines displayed higher transepithelial resistances, and consequently, were able to generate slightly higher transmural *PD*'s and higher ΔPD's in the presence of luminal glucose.

The relatively slow development of an organic solute-induced PD change in marine fish tissues was most likely due to several factors. Metabolism, as suggested by volatile activity in influx experiments and use of glucose as an energy source, may have secondarily increased the contribution of other current-generating transport systems to overall transepithelial *PD*. If the electrical polarity resulting from these metabolically-enhanced transfer processes was opposite that produced by the net movement of glucose-coupled Na flux, the time course for transepithelial PD depolarization due to Na-glucose cotransport could be relatively extended and reduced in magnitude. In higher vertebrates, intestinal ionic influx from lumen to epithelial cells through routes not related to organic solute-coupled cotransport represent approx. 90% of total cellular ionic uptake (Kimmich 1981). In marine organisms that osmoregulate and absorb monovalent ions in the upper intestine, such as marine teleosts, 90% may be an underestimate.

Addition of 2 mM D-glucose to the intestinal lumen of either herbivore or carnivore in the present study increased net sodium fluxes across the preparation from mucosa to serosa in 3 of 4 tissues used, but these increases in J_{net}^{Na} were not significant due to large variability in the unidirectional transmural fluxes (Tables 4 and 5). It is clear, however, that a strong trend for increased net cation flux to the serosa was ellicited by sugar addition to each lumen. In contrast to these results with lower vertebrates, organic solutes added to the intestinal lumen of various mammalian species markedly increase the net mucosa to serosa flow of sodium. Changes in *SCC* (ΔSCC) in surgeonfish upper intestine and both eel intestines following luminal addition of 2 mM D-glucose were significant (Tables 4, 5; $P<0.05$), and were of a nature that implied the increased net movement of cation toward the blood, supporting the tendency for elevated J_{net}^{Na} under these conditions. However, the apparent ΔJ_{net}^{Na} exhibited by each preparation was much larger than the ΔSCC displayed by the respective tissues.

In winter flounder, *Pseudopleuronectes americanus*, intestinal sodium and chloride influxes from lumen to epithelium were shown to be coupled in a 1:1 stoichiometry (Field et al. 1978). Recently, potassium was also reported to be a third binding ligand for this transport mechanism (Musch et al. 1982). This latter study also showed that the marine teleost intestine exhibits a J_{net}^{K} from serosa to mucosa and a J_{net}^{Cl} in the opposite direction. These two studies suggest that the serosa negative SCC displayed by teleost intestine in the absence of luminal organic solutes results from the following relationship:

$$SCC = J_{net}^{Na} - (J_{net}^{Cl} + J_{net}^{K}) \quad (3)$$

where serosa to mucosa potassium flux is additive with mucosa to serosa J_{net}^{Cl} in its effect on serosal negativity. If the transepithelial fluxes of these three ions are linked in a 1:1:1 stoichiometry, the

net fluxes of Na and Cl will electrically cancel, while that of K will provide the overall serosa negative polarity of the tissue. Other possible stoichiometries involving these three solutes could also produce the observed electrical character of this tissue.

Cotransport of Na with luminal glucose by an apical membrane carrier, which is independent of that serving Na−Cl−K transfer, could lead to the increased net flow of positive charge from lumen to blood, thereby reducing the magnitude of serosal negativity created by Na−Cl−K exchange alone. The significant ΔSCC brought about by the glucose addition to surgeonfish and eel intestines suggests that cotransport of sodium and glucose occurs in these tissues, but the large discrepancy between ΔSCC and the apparent ΔJ_{net}^{Na} under these conditions implies that accelerated Na−Cl−K exchange resulting from glucose metabolism also took place and reduced the depolarizing influence of coupled Na-glucose transport.

Acknowledgements. This paper was adapted from a dissertation submitted to the Graduate School of the University of Hawaii by R.P.F. in partial fulfillment of the requirements for the Ph.D. We both express our appreciation to Lester Zukeran and Steve Shimoda, Hawaii Institute of Marine Biology, for collecting the fishes used in this study.

References

Ahearn GA, Maginniss LA (1977) Kinetics of glucose transport by the perfused mid-gut of the freshwater prawn *Macrobrachium rosenbergii*. J Physiol (Lond) 271:319–336

Albus H, Heukelem JH van (1976) The electrophysiological characteristics of glucose absorption of the goldfish intestine as compared to mammalian intestine. Comp Biochem Physiol [A] 54:113–119

Ando M (1975) Intestinal water transport and chloride pump in relation to seawater adaptation of the eel, *Anguilla japonica*. Comp Biochem Physiol [A] 52:229–233

Ando M, Utida S, Nagahama H (1975) Active transport of chloride in eel intestine with special reference to seawater adaptation. Comp Biochem Physiol [A] 51:27–32

Bardach JE, Ryther JH, McLarney WO (1972) Aquaculture: the farming and husbandry of freshwater and marine organisms. Wiley-Interscience, New York

Beames CG, Merz JM, Donahue MJ (1977) Solute and water movement in the roundworm *Ascaris suum* (Nematoda). In: Jungreis AM, Hodges T, Kleinzeller A, Schultz SG (eds) Water relations in membrane transport in plants and animals. Academic Press, New York

Boge GA, Rigal A, Peres G (1979) A study of intestinal absorption in vivo and in vitro of different concentrations of glycine by the rainbow trout (*Salmo gairdneri* Richardson). Comp Biochem Physiol [A] 62:831–836

Bond C (1979) Biology of fishes. Saunders, Philadelphia

Carlisky NJ, Huang KC (1962) Glucose transport by the intestinal mucosa of the dogfish. Proc Soc Exp Biol Med 109:405–408

Cartier N, Buclon M, Robinson JWL (1979) Preliminary studies on the characteristics of phenylalanine and beta-methyl glucoside transport in the tench intestine in vitro. Comp Biochem Physiol [A] 62:363–370

Chiou JY, Ogino C (1975) Digestibility of starch in carp. Nippon Suisan Gakkaishi 41:465–466

Clarkson TW, Toole SR (1964) Measurement of short-circuit current and ion transport across the ileum. Am J Physiol 206:658–668

Cowey CB, Sargeant JR (1979) Nutrition. In: Hoar WS, Randall DJ [eds] Fish physiology, vol 8. Academic Press, New York, pp 1–69

Ferraris R (1982) Glucose and alanine transport in herbivorous and carnivorous marine fish intestines. PhD thesis, Department of Zoology, University of Hawaii, Honolulu

Field M, Karnaky KJ, Smith PL, Bolton JE, Kinter WB (1978) Ion transport across the isolated intestinal mucosa of the winter flounder *Pseudopleuronectes americanus*. I. Functional and structural properties of cellular and paracellular pathways for Na and Cl. J Membr Biol 41:265–293

Gerencser GA (1978) Enhancement of sodium and chloride transport by monosaccharides in *Aplysia californica* intestine. Comp Biochem Physiol [A] 61:203–208

Goldner AM, Schultz SG, Curran PF (1969) Sodium and sugar fluxes across the mucosal border of rabbit ileum. J Gen Physiol 53:362–363

Hofer R (1979a) The adaptation of digestive enzymes to temperature, season and diet in roach *Rutilis rutilus* and rudd *Scardinius erythrophthalmus* L. 1. Amylase. J Fish Biol 14:565–572

Hofer R (1979b) The adaptation of digestive enzymes to temperature, season and diet in roach *Rutilis rutilis* and rudd *Scardinius erythrophthalmus* L. 2. Proteases. J Fish Biol 15:373–379

Huang KC, Chen TST (1975) Comparative biological aspects of intestinal absorption. In: Csaky TZ [ed] Intestinal absorption and malabsorption. Raven Press, New York, pp 187–196

Huang KC, Rout WR (1967) Intestinal transport of sugar and aromatic amino acids in killifish, *Fundulus heteroclitus*. Am J Physiol 212:799–803

Ingham L, Arme JC (1977) Intestinal absorption of amino acids by rainbow trout *Salmo gairdneri* (Richardson). J Comp Physiol 117:323–334

Kapoor BG, Smith H, Verighina IA (1975) The alimentary canal and digestion in teleosts. Adv Mar Biol 13:109–239

Karasov W, Diamond J (1981) Intestinal glucose transport varies with taxa and diet. Am Zool 21:1030

Kimmich GA (1981) Intestinal absorption of sugar. In: Johnson L (ed) Physiology of the gastrointestinal tract. Raven Press, New York, pp 1035–1061

Kimmich GA, Randles J (1976) 2-deoxyglucose transport by intestinal epithelial cells isolated from the chick. J Membr Biol 27:363–379

Kitchin SE, Morris D (1971) The effects of acclimation temperature on amino acid transport in the goldfish intestine. Comp Biochem Physiol 40:431–443

Miller DS, Kinter WB (1979) Pathways of cycloleucine transport in killifish small intestine. Am J Physiol 237:E567–E572

Musch MW, Orellana SA, Kimberg LS, Field M, Halm DR, Krasny EJ, Frizzell RA (1982) Na−K−Cl co-transport in the intestine of a marine teleost. Nature 300:351–353

Musacchia XJ, Fisher SS (1960) Comparative aspects of active transport of D-glucose by in vitro preparations of fish intestine. Biol Bull 119:327–328

Musacchia XJ, Westhoff DD, Haaren R van (1966) Active

transport of D-glucose in intestinal segments, in vitro, of the scup *Stenotomus versicolor* and the puffer, *Spheroides maculatus*. Comp Biochem Physiol 17:93–106

Naftalin RJ, Kleinzeller A (1981) Sugar absorption and secretion by winter flounder intestine. Am J Physiol 240:392–400

Nagase G (1964) Contribution to the physiology of digestion in *Tilapia mossambica* Peters. Digestive enzymes and the effects of diets on their activity. Z Vergl Physiol 49:270–284

Ogden JC, Lobel PS (1978) The role of herbivorous fishes and urchins in coral reef communities. Environ Biol Fish 3:49–63

Oide M, Utida S (1967) Changes in water and ion transport in isolated intestines of the eel during salt adaptation and migration. Mar Biol 1:102–106

Rout WR, Lin DST, Huang KC (1965) Intestinal transport of amino acids and glucose in flounder fish. Proc Soc Exp Biol Med 118:933–938

Schultz SG, Curran PF (1970) Coupled transport of sodium and organic solutes. Physiol Rev 50:637–718

Schultz SG, Zalusky R (1964) Ion transport in isolated rabbit ileum. II. The interaction between active sodium and active sugar transport. J Gen Physiol 47:1043–1059

Shehadeh ZH, Gordon MS (1969) The role of the intestine in salinity adaptation of the rainbow trout, *Salmo gairdneri*. Comp Biochem Physiol 30:397–418

Skadhauge E (1974) Coupling of transmural flows of NaCl and water in the intestine of the eel (*Anguilla anguilla*). J Exp Biol 60:535–546

Smith MW (1966) Sodium-glucose interactions in the goldfish intestine. J Physiol 182:559–573

Utida S, Isono N, Hirano T (1967) Water movement in isolated intestine of the eel adapted to freshwater or seawater. Zool Mag (Tokyo) 76:203–204

White JR, Armstrong WM (1971) Effect of transported solutes on membrane potentials in bullfrog small intestine. Am J Physiol 221:194–201

Wilson TH (1957) In-vitro studies on intestinal absorption in fish. Biol Bull 113:362